

Mechanical elongation of astrocyte processes to create living scaffolds for nervous system regeneration

Kritika S. Katiyar^{1,2}, Carla C. Winter¹, Laura A. Struzyna^{1,3}, James P. Harris^{1,3} and D. Kacy Cullen^{1,3*}

¹Center for Brain Injury and Repair, Department of Neurosurgery, Perelman School of Medicine, University of Pennsylvania, Philadelphia, PA, USA

²School of Biomedical Engineering, Drexel University, Philadelphia, PA, USA

³Philadelphia Veterans Affairs Medical Center, Philadelphia, PA, USA

Abstract

Following brain injury or neurodegenerative disease, successful regeneration requires orchestrated migration of neurons and reformation of long-distance communication fibres, or axons. Such extensive regeneration does not occur in the mature brain; however, during embryonic development, pathways formed by glial cells extend several millimeters (mm) to create 'living scaffolds' for targeted neural cell migration and axonal pathfinding. Techniques to recapitulate long process outgrowth in glial cells have proven elusive, preventing the exploitation of this developmental mechanism for regeneration. In the current study, astrocytes were induced to form a network of interconnected processes that were subjected to controlled mechanical tension *in vitro* using custom-built mechanobioreactors. We discovered a specific micron (μm)-scale mechanical growth regime that induced elongation of the astrocytic processes to a remarkable length of 2.5 mm at an optimal rate of 12.5 $\mu\text{m}/\text{h}$. More rapid mechanical regimes ($> 20 \mu\text{m}/\text{h}$) caused greater incidence of process degeneration or outright breakage, whereas slow regimes ($< 4 \mu\text{m}/\text{h}$) led to adaptive motility, thus failing to achieve process elongation. Cellular phenotype for this astrocytic 'stretch-growth' was confirmed based on presentation of the intermediate filament glial fibrillary acidic protein (GFAP). Mechanical elongation resulted in the formation of dense bundles of aligned astrocytic processes. Importantly, seeded neurons readily adhered to, and extended neurites directly along, the elongated astrocytic processes, demonstrating permissiveness to support neuronal growth. This is the first demonstration of the controlled application of mechanical forces to create long astrocytic processes, which may form the backbone of tissue-engineered 'living scaffolds' that structurally emulate radial glia to facilitate neuroregeneration. Copyright © 2016 John Wiley & Sons, Ltd.

Received 24 February 2015; Revised 31 December 2015; Accepted 3 February 2016

Keywords astrocyte; tissue engineering; cell transplant; regeneration; neurotrauma; neurodegeneration

1. Introduction

The central nervous system (CNS) has a limited capacity to regenerate following injury or disease (Yiu and He, 2006). This lack of regenerative capability represents a huge burden, both financially and on quality of life for patients and caregivers, as each year in the USA $> 80\,000$ people

are afflicted with severe traumatic brain injury (TBI) (Gabella *et al.*, 1997), $> 500\,000$ people suffer from stroke and approximately 10 000 people acquire spinal cord injury (SCI) (Liverman, 2005). In particular, following major CNS injury, such as TBI, stroke or SCI, a major factor hindering regeneration is the formation of a glial scar consisting primarily of reactive astrocytes, which serve as a physical and chemical barrier that inhibits axon regeneration and cell migration (Fawcett and Asher, 1999).

The objective of the field of neural tissue engineering is to utilize biomaterial- and cell-based strategies to

*Correspondence to: D. Kacy Cullen, 105 E. Hayden Hall, 3320 Smith Walk, Philadelphia, PA 19104, USA.
E-mail: dkacy@mail.med.upenn.edu

augment endogenous regeneration and/or to provide direct replacement of neural cells and circuitry to promote regeneration under otherwise unfavourable conditions. This may be effectively done by mimicking developmental mechanisms. For this reason, tissue-engineered 'living scaffolds', comprised of neural cells in a preformed, often anisotropic, three-dimensional (3D) architecture, are promising for regeneration (for review, see Struzyna *et al.*, 2014). Living scaffolds possess considerable advantages over more traditional acellular biomaterial approaches through their ability to act based on feedback and crosstalk with regenerating cells/axons. They are thus able to modulate signalling based on the state and progression of the regenerative process. On this front, there are a number of promising emerging strategies for the development of regenerative scaffolds consisting of aligned glial cells (East *et al.*, 2010) and longitudinal axonal tract (Cullen *et al.*, 2012; Harris *et al.*, 2016; Pfister *et al.*, 2006; Smith, 2009; Struzyna *et al.*, 2015b). Living scaffolds have the potential to advance the field of neuroregenerative medicine by guiding the re-establishment of complex neural structures and axonal connections, potentially ultimately facilitating functional recovery following a range of currently untreatable traumatic and neurodegenerative disorders (Struzyna *et al.*, 2015a).

As the functions of glia have become better understood, there is a greater appreciation for the role of astrocytes as living 'bridges' for regenerating axons in the damaged CNS. Various studies have shown that aligned astrocytes increase and direct neurite outgrowth (Alexander *et al.*, 2006; East *et al.*, 2010), indicating that aligned astrocytes have the potential to be used as novel tissue-engineered living scaffolds to promote neuroregeneration (Alexander *et al.*, 2006; Chen and Swanson, 2003; East *et al.*, 2010; Recknor *et al.*, 2004). Indeed, supporting glial cells likely play a crucial role in regeneration (Chen and Swanson, 2003). Moreover, astrocytes and their immature precursor cells, radial glia, are among the several subtypes of glial cells that are necessary for maturation and maintenance of the CNS (Stiles and Jernigan, 2010). During development, radial glia serve as living scaffolds as immature neurons migrate along their processes extending from the germinal matrix to their final destination in the cortex. Here, neurons attach to radial glia near the ventricular zone and migrate upwards along the processes through the intermediate zone to the cortical plate. Radial glia processes span the width of the cerebral wall, which is approximately 2–4 mm in humans (Hatten and Mason, 1990). Pioneering axons are also extensively guided along glial scaffolds using their growth cones and filopodia, eventually projecting their axons along the length of the glia (Jacobs and Goodman, 1989). Additionally, radial glia serve as natural living scaffolds in the spinal cord by acting as a guide for developing axons during the formation of the corticospinal tract (Joosten and Gribnau, 1989), as well as maintaining the white matter pattern of the spinal cord during development (Stiles and Jernigan, 2010). Studies have shown that radial glia

may promote neuronal migration and axonal regeneration (Filous *et al.*, 2010; Mattotti *et al.*, 2012). However, radial glia are primarily present early during development, and differentiate into stellate astrocytes and neurons by adulthood (Leavitt *et al.*, 1999).

A critical feature of these developmental glial scaffolds is their long processes, spanning several mm and across multiple layers of the cortex; however, there has yet to be a tissue culture technique capable of recapitulating this astrocyte morphology. The objective of the current study was to create astrocytes with ultra-long processes to structurally mimic the radial glial living scaffolds seen in development. This was achieved by utilizing controlled mechanical tension in custom-built mechanobioreactors to create constructs consisting of ultra-long, aligned glial processes, to morphologically emulate radial glia. Here, we modified previously established procedures that apply mechanical tension to induce axon stretch growth *in vitro* (Pfister *et al.*, 2004; Smith, 2009), and we identified a specific mechanical regime that allowed for controlled 'stretch-growth' of astrocytic processes. In future studies, these ultra-long, aligned astrocyte processes may form the backbone of tissue-engineered living scaffolds, emulating the structure of radial glia seen in development, to promote regeneration following CNS injury or disease.

2. Materials and methods

2.1. Primary cortical astrocyte isolation and culture

Astrocytes were harvested from postnatal day 0 or day 1 (P0–P1) Sprague–Dawley rat pups, as described previously (Cullen *et al.*, 2007b, 2011). Briefly, the brains were isolated and microdissection techniques were employed to remove the meninges and all subcortical structures, leaving just the cerebral cortices. This tissue was minced and then dissociated with 0.25% trypsin + EDTA, followed by 0.15–0.30 mg/ml DNase diluted in Hanks's balanced salt solution (HBSS), and triturated to separate the tissue. The suspension was then centrifuged at 1000 rpm for 3 min, and cultured in Dulbecco's modified Eagle's medium (DMEM)/F-12 medium supplemented with 10% fetal bovine serum (FBS) and plated in flasks (Cullen *et al.*, 2007b). Over the first few weeks, cultures were maintained by mechanically agitating the flasks prior to changing the medium, in order to dislodge and remove less adherent cell types, and the astrocytes were passaged at 90% confluency and replated at 30 000 cells/cm² (McCarthy and de Vellis, 1980). These methods have previously been shown to produce a nearly pure population of astrocytes (> 95%) (Cullen *et al.*, 2007b; McCarthy and de Vellis, 1980), which we verified in our cultures using immunocytochemistry, as described below (data not shown). Between passages 2–8, the astrocytes were replated in a serum-free medium to induce a mature glial phenotype, as described below. This defined medium consisted of neurobasal medium

Elongation of astrocyte processes for nervous system regeneration

supplemented with 0.25% L-glutamine, 2% B-27 and 1% G-5, at a seeding density in the range of 40 000–125 000 cells/cm². To determine the effect of substrates on astrocyte growth and process formation, four substrates were tested prior to stretch: polystyrene ($n = 4$); thick ACLAR 33C film (199 μm ; $n = 4$); 1 mg/ml Matrigel on thick ACLAR 33C film ($n = 4$); and 1 mg/ml rat-tail collagen type I on thick ACLAR 33C film ($n = 4$). Polystyrene and ACLAR 33C in all groups were coated with 0.20 $\mu\text{g}/\text{ml}$ poly-L-lysine (PLL) overnight, then rinsed prior to the addition of Matrigel or collagen I coating. The Matrigel and collagen I coatings were extremely thin to ensure sufficient cell adhesion to the membranes, in order to withstand the eventual mechanical forces that would be applied to the cells for stretch-growth studies. These thin ECM coatings were achieved by adding 10 μl substrate and spreading it evenly across the culture surface (approximately 2 cm²), using the pipette tip, prior to gelation.

2.2. Primary cortical neuron isolation and culture

Cerebral cortices were extracted from embryonic day 18 Sprague–Dawley rats (Charles River) and dissociated to isolate cortical neurons, as described (Struzyna *et al.*, 2015b). Following dissociation, neurons were resuspended at $2\text{--}4 \times 10^5$ cells/ml in defined co-culture medium (neurobasal medium +2% B-27, 1% G-5 and 0.25% L-glutamine). To assess the interaction between neurons and stretched astrocyte processes, approximately 10–20 μl neuronal solution was added to the cultures containing stretched astrocytes; however, the neurons were added some distance away from the processes in order to enable the assessment of neuronal migration onto the ‘stretch-grown’ astrocyte processes.

2.3. Cortical astrocyte culture and process ‘stretch-growth’ using custom-built mechanobioreactors

Astrocytes were plated in custom-built mechanobioreactors consisting of a custom-designed process expansion chamber, linear motion table, stepper motor and controller. The expansion chamber, made of polyether ether ketone (PEEK), serves as a housing for the cells and consists of a sealed enclosure with a port for CO₂ exchange, a removable process stretching frame (known as the carriage) and connecting rods to apply displacements. The carriage was designed to slowly divide two populations of cell somata, thereby stretching their interconnecting processes. The carriage arranges two adjoining substrates in an overlapping fashion on which cells are cultured (Figure 1). The bottom substrate (199 μm thick), made of optically transparent ACLAR 33C film, covers the entire bottom of the stretching frame on which a stationary population of astrocytes was cultured. The plating area within the

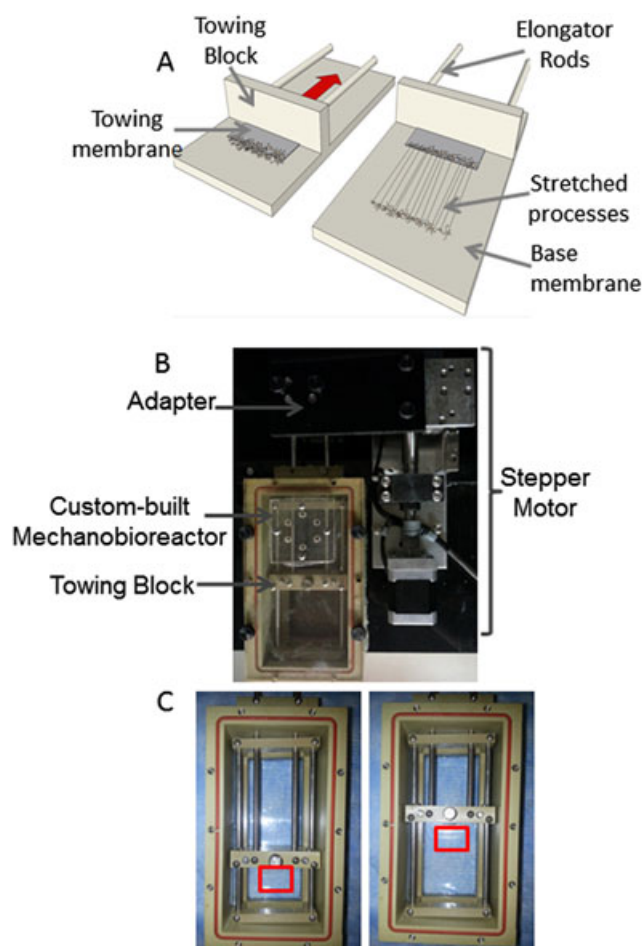


Figure 1. Development of astrocyte living scaffolds via stretch-growth. (A) Astrocytes were plated in a custom-built mechanobioreactor attached to (B) A micro-stepper motor in order to apply controlled mechanical tension. (C) The cells were plated along the interface of two overlapping transparent membranes: a stationary membrane and a towing membrane (outlined with red box). The towing membrane was attached to a block at its original position, then was gradually pulled back as the driving rods were pulled by the micro-stepper motor attached to them. As the towing membrane was pulled back at the desired rate, the network of processes that had formed in static culture were stretched, due to the applied tension. This resulted in long, aligned processes

mechanobioreactor is 15 \times 8 cm. An overlapping movable substrate (a thinner ACLAR 33C film, 19 μm thick) was placed on top of the bottom ACLAR substrate and served as the substrate for the moving population of cells (referred to as the towing membrane). Processes were mechanically stretched by forces transduced from a stepper motor via attachment to the connecting rods, with the entire assembly mounted to a fixed linear motion table. In turn, the rods displace the stretching frame with 0.5 μm accuracy. The system is computer controlled by a programmable stepper motor indexer, which is controlled using a custom-written LabView 2011 Run-time Engine program.

Cells were plated at a density of 40 000–125 000 cells/cm² along the interface of the two membranes: the 199 μm -thick ACLAR 33C base membrane and the thin 51 μm or ultra-thin 19 μm transparent ACLAR 33C

towing membrane, which was polished further to reduce thickness. The base and towing membranes were etched with 1 N NaOH and the base membrane was adhered to the bottom of the carriage, while the towing membrane was adhered to the towing block, and this entire carriage assembly was placed within the PEEK mechanobioreactors enclosure. The plating area was then coated with 0.05 mg/ml poly-L-lysine (PLL; BD Biosciences) overnight, rinsed, coated with 1 mg/ml rat tail collagen type I (BD Biosciences) at 37°C and allowed to incubate overnight. Astrocytes were then plated and allowed to adhere for 45 min before flooding the mechanobioreactor with defined medium. Approximately 4–5 days after plating, the mechanobioreactor was connected to the stepper motor and mechanical tension was applied to the cells spanning the membranes, by gradually pulling the towing membrane back at a rate of 0.1, 0.3 or 0.5 mm/day (corresponding to 4.17, 12.5 and 20.8 $\mu\text{m/h}$).

2.4. Microscopic analysis and immunocytochemistry

The astrocyte cultures were routinely imaged using phase-contrast microscopy techniques on a Nikon Eclipse Ti-S inverted microscope with Nikon Elements Basic Research software. For immunocytochemistry analysis, astrocyte cultures were fixed in 4% formaldehyde for 30 min, rinsed in phosphate-buffered saline (PBS) and permeabilized using 0.3% Triton X-100 plus 4% horse serum for 60 min. Primary antibodies were added (in PBS + 4% serum solution) at 4°C for 12 h. Primary antibodies to identify astrocytes and neurons were used. Rabbit anti-glia acidic fibrillary protein (GFAP; Millipore AB5804) was used to identify the intermediate filament protein present in astrocytes, and mouse anti- β -tubulin III (Sigma, C8198) was used to identify an element of microtubules expressed in neurons. After rinsing, Alexa 561 donkey anti-rabbit IgG and Alexa 488 donkey anti-mouse IgG secondary antibodies (1:500 in PBS + 4% serum) were added at 18–24°C for 2 h. Stretched or static astrocytic cultures were fluorescently imaged, using a laser-scanning confocal microscope (LSM 710 on an Axio Observer Z1; Zeiss, Oberkochen, Germany). For each culture, multiple confocal *z*-stacks were digitally captured and analysed.

2.5. Quantification of stretched astrocytic processes and statistical analysis

Features of stretch-grown astrocyte somata/processes were quantified from phase-contrast micrographs (acquired as described above) of astrocyte cultures following mechanical tension-induced growth. Areas of stretch-growth that exhibited a dense cabling of somata/processes were termed ‘bundles’, and more spread-out regions where individual stretched somata and processes

could be seen were considered dispersed ‘regions’. The number of stretch-grown bundles and regions within each stretched culture was quantified from astrocyte cultures subjected to mechanical displacements at rates of 4, 12.5 and 20.8 $\mu\text{m/h}$ ($n = 4$, $n = 30$, $n = 20$ cultures/rate, respectively). Also, across stretch rates of 12.5 and 20.8 $\mu\text{m/h}$, the number of processes/somata within the bundles or regions were quantified and a box-whisker-plot was produced, using the statistical software package Stata (College Station, TX, USA). One-way analysis of variance (ANOVA) was used to analyse differences in the number of ‘dense bundles’ vs ‘dispersed regions’ of astrocyte stretch-growth formed/mm towing membrane, as a function of stretch rate (4, 12.5 and 20.8 $\mu\text{m/h}$). When significant differences were found, a *post hoc* Tukey comparison test was performed. For all statistical tests, $p < 0.05$ was required for significance.

3. Results

3.1. Media and substrate optimization of immature astrocyte culture for stretch

In order to induce stretch-growth in astrocytic processes, it was essential that the astrocytes display a robust process-bearing morphology. Astrocytes are conventionally cultured in a serum-containing medium, resulting in a flat, brick-like morphology with few processes. This represents an immature, proliferative state (Figure 2a). In contrast, we found that astrocytes cultured in defined medium exhibited a more mature, process-bearing morphology (Figure 2b) and absent overt proliferation. These process-bearing astrocytes were cultured on four different substrates to determine the effect of the substrate on astrocyte morphology and health. The substrates were polystyrene, Aclar alone, Aclar coated with Matrigel (1 mg/ml) or collagen type I (1 mg/ml). Although process-bearing morphology was observed when astrocytes were cultured on all four substrates in serum-free medium, more robust processes, clustering and network formation were found when astrocytes were cultured on Matrigel (Figure 2e) or collagen type I (Figure 2f–h), as compared to cultures on polystyrene (Figure 2c) or ACLAR alone (Figure 2d). Long-term survival of the desired morphology, as well as clustering, was confirmed up to 20 days *in vitro* when cultured on collagen I (Figure 2h), which was necessary, as the technique of stretch-growth requires cells to survive *in vitro* for several weeks. We have previously found that cell clustering is advantageous to stretch-grow processes, which require robust networks that span the towing membrane and base membrane. With minimal clustering, as seen when astrocytes were cultured on polystyrene or ACLAR 33C film alone, the astrocytes would likely be unable to sustain the applied mechanical tension. Based on these findings, collagen type I was used to coat the towing membrane and

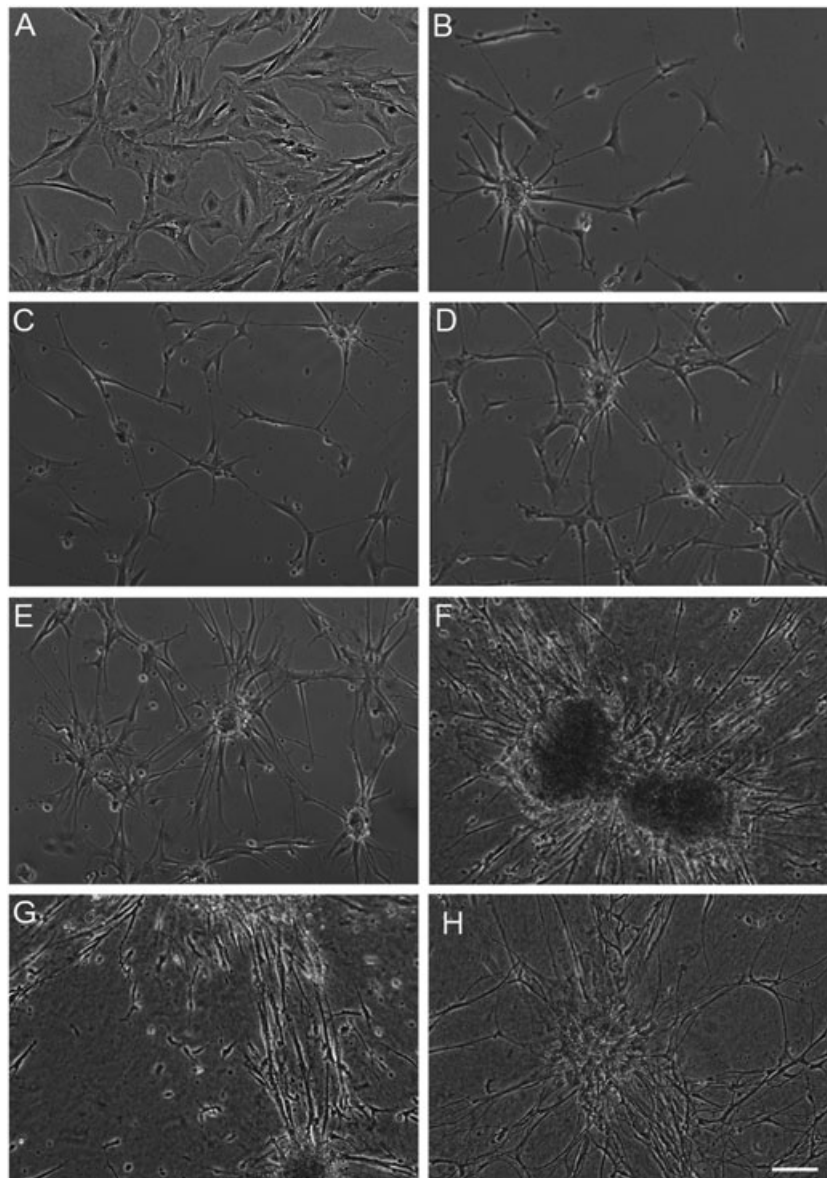


Figure 2. Optimization of culture conditions resulted in astrocytic clustering and numerous processes. Brightfield microscopy images of astrocytes cultured on polystyrene in (A) serum-containing medium (DMEM/F12 + 10% FBS) vs (B) defined, serum-free medium (neurobasal +2% B27 + 1% G-5 + 0.25% L-glutamine) produced astrocytes with a mature, non-proliferative, process-bearing morphology. Astrocytes cultured for 5 days *in vitro* (substrates precoated with poly-L-lysine), grown on (C) polystyrene only, (D) ACLAR only, (E) 1 mg/ml Matrigel-coated ACLAR and (F) 1 mg/ml rat tail collagen type I-coated ACLAR. (C-F) Cultures were plated with defined media and astrocytes cultured on rat tail collagen type I showed the most robust clustering and processes at both (G) 5 and (H) 20 days *in vitro*; scale bar =100 μ m

stationary base in all subsequent studies. To determine whether the astrocytic processes plated on the towing membrane were able to cross the interface and form a network of processes with astrocytes on the base membrane, astrocytes in defined medium were cultured along the interface of two membranes in static (i.e. non-stretch) conditions. Here, the membranes were ACLAR 33C, with a 19 μ m thick membrane (representing the ‘towing’ membrane in the mechanobioreactors) resting on top of a 199 μ m-thick base membrane. We found that astrocytes plated on collagen type I were able to extend processes that crossed the interface between these membranes, and exhibited robust growth (Figure 3).

3.2. The application of continuous mechanical tension produced long, aligned astrocytic processes

Astrocytes were cultured under serum-free, static conditions in the mechanobioreactors for 4–5 days *in vitro* to allow network formation between the cell populations on either side of the towing-base membrane interface. This resulted in robust astrocyte growth spanning the cell populations on either side of the interface, before the application of mechanical tension (Figure 4a). After this static period, the micro-stepper motor was engaged to continuously displace the towing membrane in sub- μ m increments, thus applying external tensile forces to the

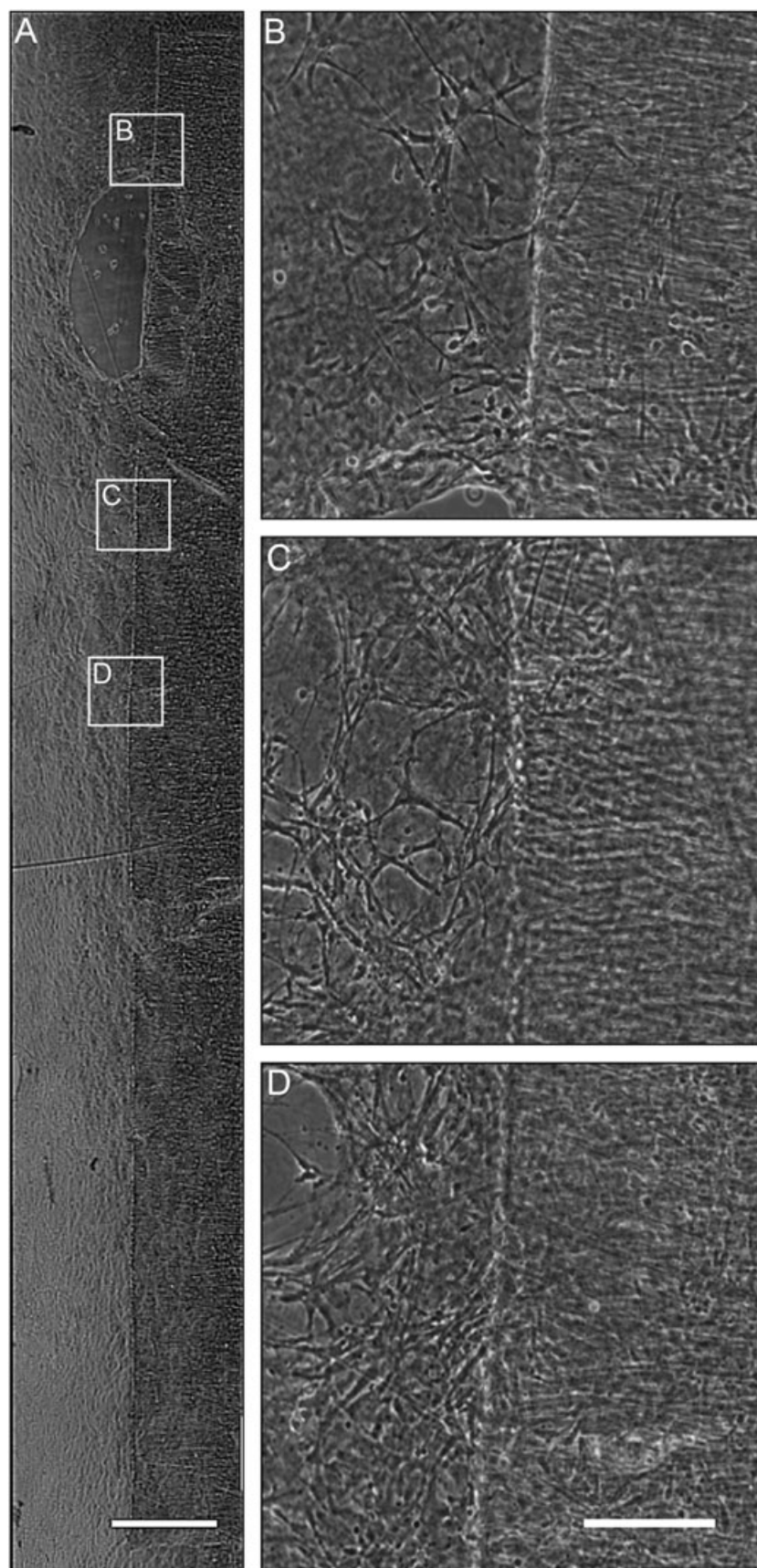


Figure 3. Astrocytes plated across ACLAR 33C towing membrane resulted in robust astrocytic network formation across the interface. Brightfield microscopy images of astrocytes 1 day *in vitro* on the collagen I-coated interface between the thin ACLAR 33C towing membrane and the thicker ACLAR base membrane with defined media. (A) Brightfield image of process-bearing astrocytes growing along the entire towing membrane. Scale bar = 300 μm . (B, C, D) Higher-magnification insets showing processes crossing the towing membrane interface. Scale bar = 50 μm

Elongation of astrocyte processes for nervous system regeneration

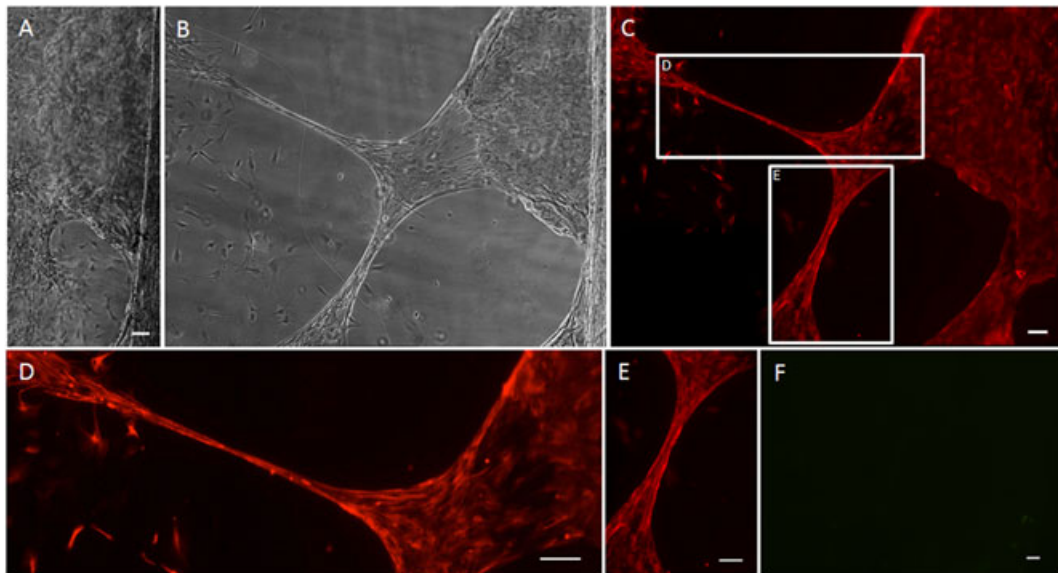


Figure 4. Stretched astrocyte processes express glial fibrillary acidic protein (GFAP). After the application of continuous mechanical tension at a rate of 0.3 mm/day (12.5 $\mu\text{m}/\text{h}$), astrocyte processes were successfully ‘stretch-grown’. (A) Brightfield image of culture prior to application of continuous mechanical tension; scale bar = 50 μm . (B) Brightfield image of the same area from (A) after stretch. (C) Fluorescence image of the same area, showing labelling for GFAP in red, confirming the astrocytic phenotype of the stretch-grown cells and processes; (D, E) enlargements of the stretched regions from (C). (F) Fluorescence of the same area from (B), showing absence of labelling for β -tubulin III in green, demonstrating that there were no contaminating neurons/neurites in the culture; scale bar (C-F) = 100 μm

cells and processes spanning the towing and base membranes. Application of constant mechanical tension at a rate of 0.3 mm/day (12.5 $\mu\text{m}/\text{h}$) for several days produced long astrocytic somata and processes, spanning several hundred μm to several mm in length (Figure 4b). As this is the first report of mechanical elongation of processes in astrocyte cultures, it was crucial to verify that the phenotype of the stretch-grown processes was indeed astrocytic. Immunocytochemistry and fluorescent microscopy of stretch-grown cells and processes revealed complete expression of the astrocytic marker, GFAP, but not the neural marker β -tubulin III (Figure 4), confirming that the cells were of astrocytic lineage and not a contaminating cell type (i.e. neurons, fibroblasts, etc.).

The effects of alternative stretch-growth regimes were also investigated. After constant mechanical tension had been applied to the processes network at a rate of 0.5 mm/day (20.8 $\mu\text{m}/\text{h}$), a highly organized process alignment with parallel intercellular orientations was observed at 1 day. However, this response was heterogeneous across the length of the towing membranes in the cultures (Figure 5). By applying further mechanical tension at this rate, extreme stretch-growth of the processes was observed. Here, applied displacement at a rate of 0.5 mm/day for several days caused the astrocytic processes to lengthen on the order of 1.5 mm (Figure 6a, b), with maximal achieved lengths of 2.5 mm to date. As seen with the initial stretching, after mechanical tension had been applied for longer durations the response was heterogeneous across the towing membrane. For instance, mm-scale elongated astrocyte processes were found scattered in discrete locations, with more robust stretch seen along the corners of the towing membrane

(Figure 6b), which may have been due to the increased surface area of the towing membrane–base interface.

We observed that areas of astrocyte stretch-growth fell into one of two descriptive categories: (a) long, dense cables of somata/processes, which we termed ‘bundles’ (Figure 7a–c); or (b) more spread-out regions, where individual stretched somata and processes could be seen, which we describe as dispersed ‘regions’ (Figure 7d). The numbers of stretch-grown bundles and regions/mm towing membrane were quantified from astrocyte cultures subjected to growth rates of 4, 12.5 and 20.8 $\mu\text{m}/\text{h}$. The total number of stretch-grown areas varied significantly, based on rate ($p < 0.05$), with rates of 12.5 and 20.8 $\mu\text{m}/\text{h}$ each significantly differing from displacement rates of 4 $\mu\text{m}/\text{h}$ ($p < 0.05$), although these rates did not vary from each other (Figure 7). Indeed, cultures subjected to towing membrane displacement at a rate of 4 $\mu\text{m}/\text{h}$ were devoid of stretch-grown processes. Conversely, stretch-grown bundles and regions were readily apparent across the length of towing membrane displaced at rates of 12.5 or 20.8 $\mu\text{m}/\text{h}$. At a rate of 12.5 $\mu\text{m}/\text{h}$, 75% of the stretch-grown areas were dispersed regions, whereas 25% were dense bundles. At a higher rate of 20.8 $\mu\text{m}/\text{h}$, 69% of stretch-grown areas were dispersed regions and 31% formed dense bundles (Figure 7e). However, there was a 25% increase in the total area of process stretch-growth when mechanical tension at a rate of 12.5 $\mu\text{m}/\text{h}$ was applied, as compared to 20.8 $\mu\text{m}/\text{h}$. Across these successful stretch rates of 12.5 and 20.8 $\mu\text{m}/\text{h}$, the number of processes/somata within the bundles or regions were quantified. When stretch-grown bundles were formed, they consisted of 1–17 individual somata/processes (mean 8.08, SD 4.51), whereas the

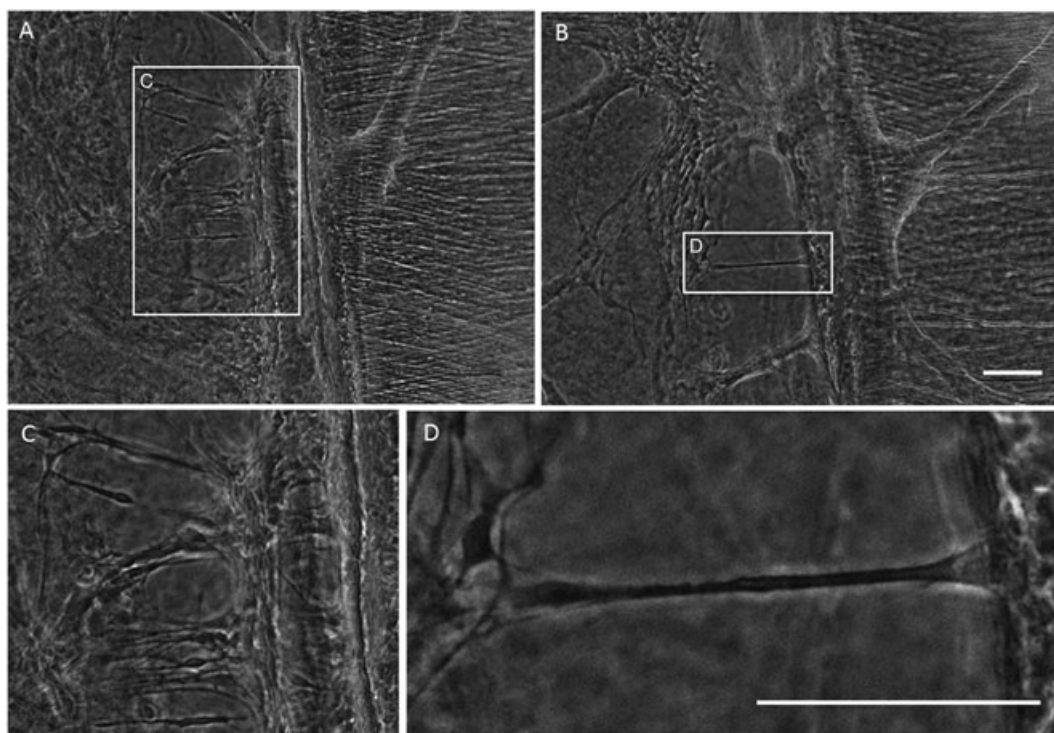


Figure 5. Constant mechanical tension induces 'stretch-growth' and organized alignment of astrocytic processes. Application of constant mechanical tension produces early stretched processes and process alignment (outlined with white box) orthogonal to the towing membrane and parallel to the direction of applied tension by 1 day post-stretch. Scale bars = 100 μ m

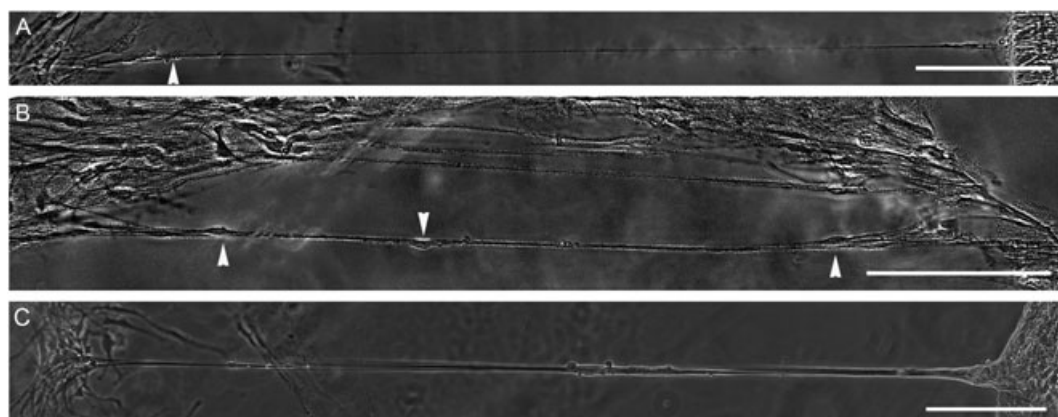


Figure 6. Constant mechanical tension causes astrocytic processes to grow up to several mm in length. After allowing astrocytes to form networks across the collagen type I-coated membrane interface for 3 days, the networks were mechanically grown at a rate of 0.5 mm/day (20.8 μ m/h) for 5 days. (A, B) These images demonstrate astrocyte processes up to 1.3 mm in length; arrowheads indicate cell bodies. (C) Robust stretch-growth processes were often seen at the corner of the towing membrane. Scale bars = 200 μ m

larger regions of stretch-growth contained 19–123 individual somata and processes (mean 64.0, SD 39.1) (Figure 7f).

3.3. Effect of stretch rate on the health and morphology of astrocytic processes

In order to find an optimal rate of applied tension to induce process stretch-growth, we examined rates in the range 0.1–0.5 mm/day (4.17–20.8 μ m/h). A stretch rate of 0.3 mm/day (12.5 μ m/h) for 5 days most consistently resulted in healthy stretched processes during the initial

phase of growth (Figure 8a). While a higher stretch rate (0.5 mm/day or 20.8 μ m/h) yielded healthy-appearing stretched processes, it also resulted in the appearance of some unhealthy stretched processes, displaying early signs of degeneration, with debris build-up along the processes (Figure 8b, c), and eventually spotted disintegration of the processes (Figure 8d). It should be noted that some processes held up to this high rate and maintained a healthy appearance, while others displayed a degenerating morphology. In contrast, when the rate of stretch was decreased to 0.1 mm/day (4.17 μ m/h) for 10 days, yielding a potential stretch length of 1 mm, no regions of stretch-growth were seen and evidence of

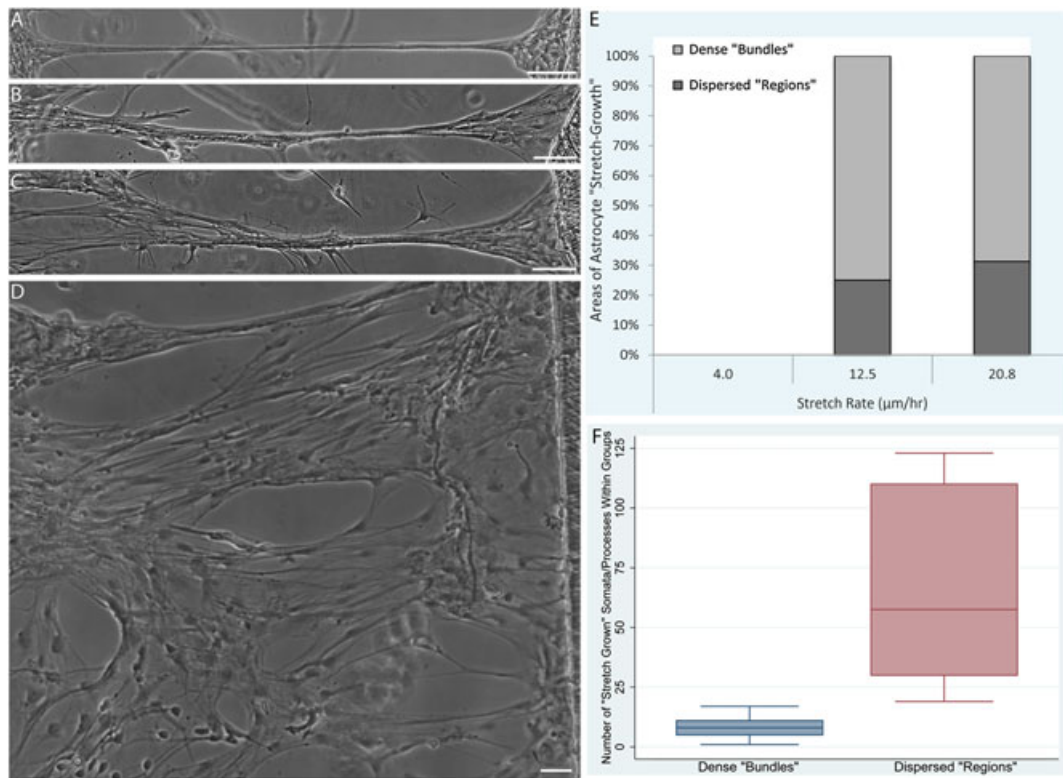


Figure 7. Stretched astrocytic processes may form dense bundles or present as more dispersed 'regions'. (A–C) The majority of stretched astrocytic processes formed dense bundles consisting of multiple individual astrocyte somata/processes. (D) Larger dispersed 'regions' of more spread-out stretch-growth were also observed. (E) The breakdown of the incidence of stretched 'bundles' vs 'regions' was quantified, revealing a dependence on stretch rate ($p < 0.05$), with an absence of stretch regions at $4 \mu\text{m/h}$ and similar proportions of 'bundles' and 'regions' at 12.5 and $20.8 \mu\text{m/h}$. (F) The number of individual astrocyte somata and processes comprising the 'bundles' vs 'regions' was also quantified, revealing that 'bundles' consisted of 8.08 ± 4.51 (range 1–17) astrocytes, whereas 'regions' consisted of 64.0 ± 39.1 (range 19–123) astrocytes. Data are presented as mean \pm SD, with quantification from $n = 10$ 'stretch-grown' cultures. Scale bars = $100 \mu\text{m}$

process degeneration was also not observed (data not shown). This can likely be explained due to 'adaptive motility' in the astrocytes, where they were able to migrate with the towing membrane instead of remaining adhered and stretching when mechanical tension was applied.

3.4. Neurons survive and extend neurites directly along stretched astrocytic processes

Once astrocyte processes had been subjected to tension-induced growth, neurons were added to the culture, some distance away from the bundles of stretch-grown processes. The neurons were allowed to grow for 3 days *in vitro*, and then the co-cultures were fixed and labelled for GFAP to identify astrocytes, β -tubulin III to label neurons, and a Hoechst counterstain to label the nuclei (Figure 9). The stretch-grown astrocytes were clearly seen to be dense bundles of multiple somata and processes. Importantly, seeded neurons were observed readily adhered to these elongated astrocyte process bundles, despite being seeded several mm away, suggesting migration along the astrocyte processes. Moreover, neurons robustly extended neurites directly along, and in alignment with, the stretch-grown astrocytic processes (Figure 9).

4. Discussion

Due to the limited capacity for CNS regeneration, neurotrauma and neurodegenerative diseases lack effective treatment options. In these cases, successful regeneration would involve a precisely orchestrated re-establishment of neural connections and reformation of cellular structure, often requiring directed long-distance axonal growth and cellular migration. During CNS development, long distance pathways are naturally formed by radial glial cells to facilitate targeted neural cell migration and axonal pathfinding. Our objective was to create tissue-engineered 'living scaffolds' for neuroregeneration by emulating developmental mechanisms. Here, we created constructs that consist of long astrocyte processes that structurally mimicked radial glia. To accomplish this, we first optimized culture conditions to induce a process-bearing morphology in secondary cortical astrocytes. Several culture substrates were tested to produce robust process outgrowth, network formation and clustering. The ACLAR 33C film used as the base of the mechanobioreactor showed robust process outgrowth when coated with Matrigel and collagen I, which have been implemented for 3D neuronal-astrocytic co-cultures and 3D gels for astrocyte alignment, respectively (Cullen

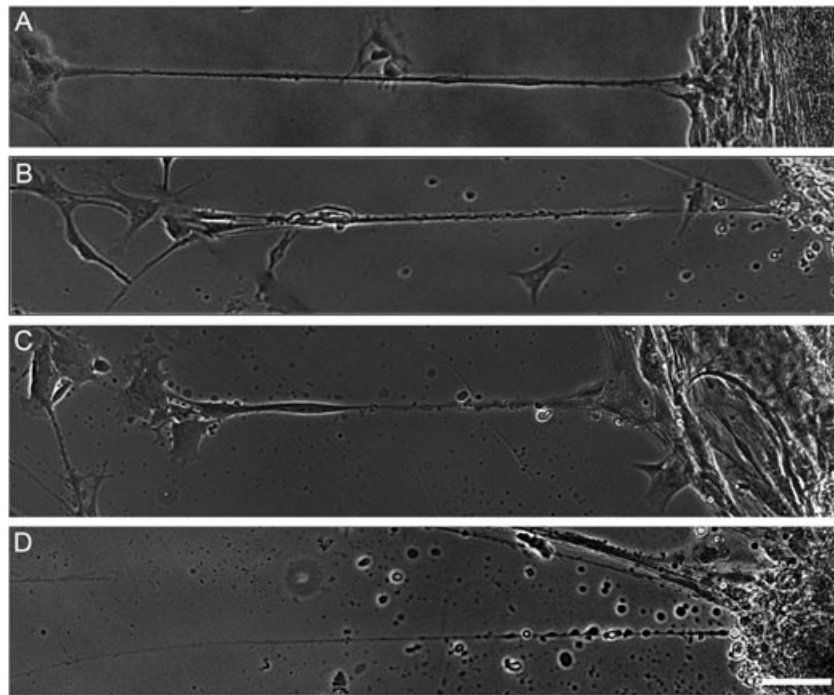


Figure 8. Astrocyte process health is dependent on stretch rate. (A) Healthy ‘stretch-grown’ astrocyte processes displayed consistent diameter and structure along the length. (B) Astrocyte process displayed early signs of degeneration, with irregular diameter and ‘beading’ becoming apparent along the process. (C) Unhealthy ‘stretch-grown’ astrocyte processes underwent degeneration, as evident by the increased ‘beading’ along the length and early disintegration of the process. (D) Degenerated astrocyte processes exhibited severe ‘beading’ and overt disintegration. Scale bar = 200 μm

et al., 2006, 2007a, 2007b, 2007c, 2011; East *et al.*, 2010; Irons *et al.*, 2008; Vukasinovic *et al.*, 2009). Astrocytes showed most robust process outgrowth and clustering when cultured on collagen I, but similar results were observed when cultured on Matrigel. Matrigel is primarily composed of laminin and collagen IV, with additional proteoglycans and a host of growth factors. Given these stark differences between collagen I and Matrigel, it is surprising that we observed similar degrees of astrocytic growth, clustering and network formation. Even though previous studies have successfully cultured and aligned astrocytes on laminin-coated substrates (Pixley *et al.*, 1987; Recknor *et al.*, 2004), we have found reduced astrocyte process outgrowth and survival on laminin substrates (data not shown). These effects are likely attributed to differences in the type of integrin receptors expressed on astrocytes, which varies depending on the developmental stage, with certain receptors highly expressed during the radial glia stage and others more highly expressed later in development (Scemes and Spray, 2011). Optimizing culture conditions to obtain a robust process-bearing morphology was crucial to successful astrocytic stretching. Previous studies have shown that a network of axons is necessary prior to the application of mechanical tension, in order to successfully stretch-grow axons (Pfister *et al.*, 2004, 2006; Smith, 2009). Likewise, we needed to induce the formation of a network of astrocytic processes with sufficient resilience and growth capacity to respond to the applied mechanical loading. Other studies have found that the addition of factors such as fibroblast growth factor (FGF) increases in cyclic AMP, and freeze–thawing cells

yields long astrocytic processes (Gaul and Lubbert, 1992; Yu *et al.*, 2006). However, the induction of a process-bearing morphology by freeze–thawing astrocytes in culture revealed no significant morphological difference compared to our simpler method of culture in defined, serum-free medium. Moreover, changes in medium composition alone were not expected to produce processes as long as we have obtained through stretch-growth (up to 2.5 mm). Over days *in vitro*, the populations of astrocytes across the towing and base membranes became interconnected, due to outgrowth of the astrocyte processes. The somatic clustering and process-bearing morphology was maintained long-term, as the stretch-growth process takes several days to weeks to accomplish *in vitro*. The astrocytes were plated in a random fashion, and we found that as seeding density increased, the density of the astrocytic networks across the membranes also increased. While increasing the number of cells certainly increases the probability that the desired orientation and network formation will occur, cell–cell interactions among the astrocytes may also play a role (Jacobs and Goodman, 1989).

Custom-built mechanobioreactors were then utilized to apply gradual, controlled mechanical tension to the processes spanning the astrocyte populations. Application of mechanical tension yielded heterogeneous stretch within cultures, with the most robust stretch seen near the corners of the towing membranes. The thickness of astrocytic processes after stretch varied, with some processes being finer than others, underscoring the heterogeneous effects of mechanical tension on the processes. This could be a

Elongation of astrocyte processes for nervous system regeneration

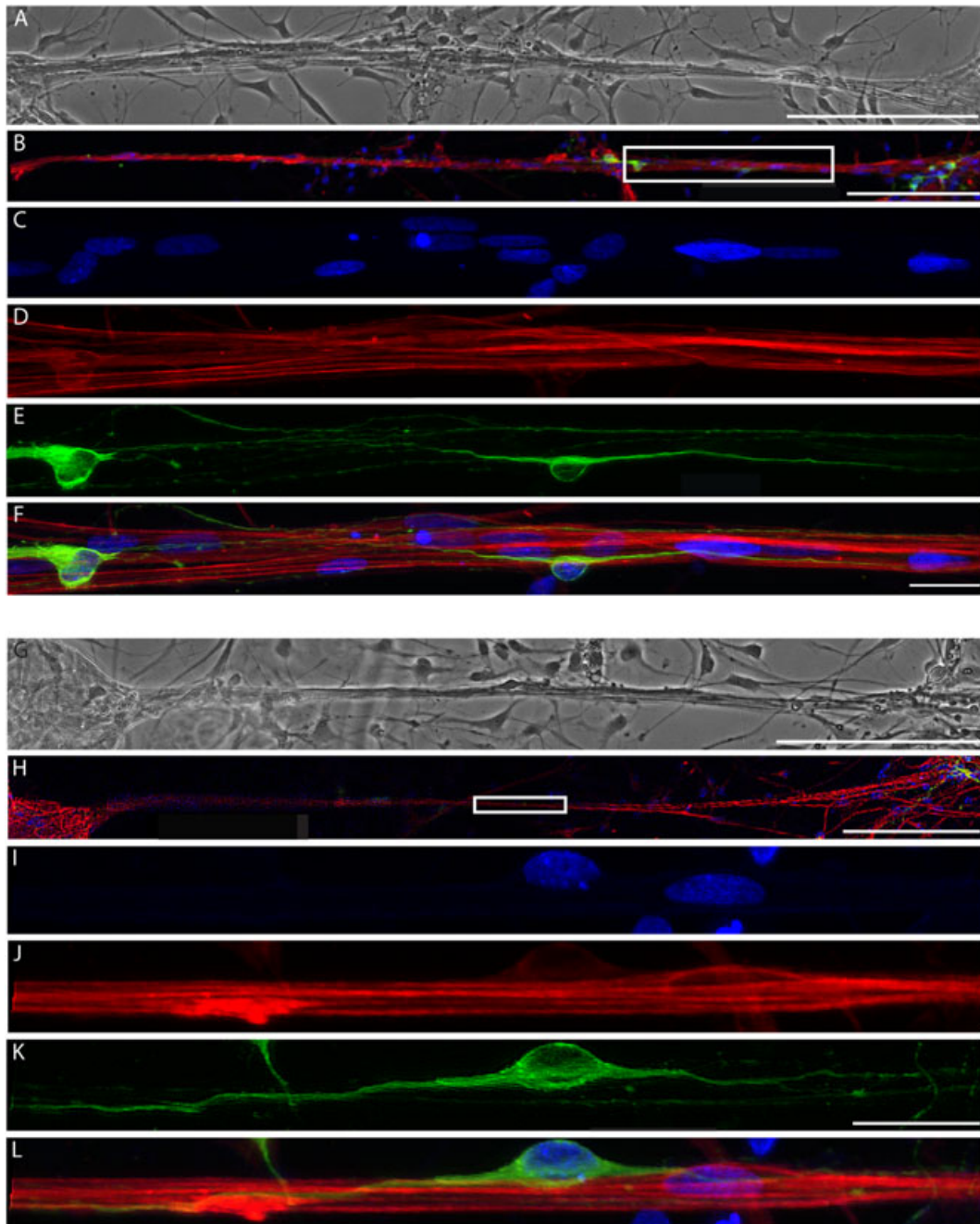


Figure 9. Neurons extend neurites directly along the stretched astrocytic processes. (A, G) Phase-contrast image and (B, H) confocal reconstruction of two separate areas of astrocytic processes that were stretched to unprecedented lengths of 1.5 mm and directed and supported neuronal survival; scale bars = 200 μm . (C–F) Enlargement of boxed region in (B), showing (C) Hoechst counterstain, (D) GFAP-positive stretched astrocytic processes, (E) β -tubulin III-positive neurons and (F) overlay; scale bars = 25 μm . (H) Second area demonstrating stretched astrocytic bundles seeded with neurons were (I) stained for Hoechst, (J) labelled for GFAP, (K) β -tubulin III (Tuj1) and (L) overlay

natural result of the random astrocyte plating and network formation prior to stretching. For example, the majority of stretched processes formed dense ‘bundles’; however, there were also a considerable number of larger regions consisting of groups of individual somata and processes. These engineered astrocyte architectures recapitulate aspects of radial glia that promote neuronal migration from the subventricular zone to the cortical plate during development. These architectures also morphologically mimic features of the glial tube in the rostral migratory

stream which promotes neuronal/stem cell migration from the subventricular zone to the olfactory bulb. Therefore, this novel mechanism of astrocytic process elongation and alignment structurally mimics developmentally relevant neural architectures that are known to promote neural cell migration *in vivo*.

The rate at which mechanical tension was applied affected the health of the stretched processes and their ability to stretch, with high rates leading to degeneration of some processes and low rates leading to individual

cells removing adhesions from one of the membranes, an example of adaptive motility. For instance, Zhou *et al.* (1990) found that astrocytes can migrate up to $9.17 \mu\text{m}/\text{h}$ ($220 \mu\text{m}/\text{day}$), suggesting that astrocytes in the system may respond to a slower stretch regime by actively disengaging from one of the membranes. Accordingly, we found more successful and robust stretched astrocytic processes when mechanical tension was applied at a rate of $12.5 \mu\text{m}/\text{h}$, a rate slightly faster than that reported for astrocyte migration. Moreover, the maximum stretch rate tolerated by astrocytes is significantly smaller than that used for dorsal root ganglia (DRG) axon elongation, previously reported using the same system. For example, Pfister *et al.* (2004) reported an applied stretch rate of $1 \text{ mm}/\text{day}$ ($41.7 \mu\text{m}/\text{h}$) for the first 24 h, gradually increasing the rate to $4 \text{ mm}/\text{day}$ ($166.7 \mu\text{m}/\text{h}$), which was sustained for several weeks (Pfister *et al.*, 2004). The increased tolerance for stretch-growth of DRG axons is likely due to the inherent capability of these cells to undergo stretch in the body during development, e.g. *in utero*, but also as the limbs lengthen during postnatal development and into adulthood (Pfister *et al.*, 2006; Smith, 2009). Likewise, it is probable that radial glia undergo some form of stretch-growth as the cortex expands in early embryonic development. While mechanical elongation of astrocytic processes has been suggested, based on tissue swelling in response to nitrocellulose implants (Jaeger, 1988), our study is the first to show the direct application of controlled mechanical forces to induce process elongation *in vitro*. The stretched processes were confirmed to be of astrocytic origin (rather than being neurites from contaminating neurons) by labelling for the intermediate filament GFAP (Figure 4c–e) that is highly expressed in astrocytes. Although astrocytes subjected to this mechanical growth regime structurally emulate radial glia, we have yet to assess whether the astrocytes phenotypically revert back to radial glial cells due to the application of mechanical tension. Further studies including a detailed phenotypic assessment will be required to determine whether these stretch-grown astrocytes exhibit markers of immature astrocytes and/or radial glia. Interestingly, our work identified a unique mechanical growth regime – occurring in μm -scale increments sustained over days – that induced elongation of astrocytic processes, yielding cultures consisting of long aligned processes measuring up to 2.5 mm , with the potential for greater lengths to be achieved in the future. It is remarkable that we induced a process-bearing morphology and mechanically elicited process elongation using CNS astrocytes, which generally lose their process-bearing morphology when cultured *in vitro* and do not naturally undergo large-scale stretch in the body. This likely explains the relatively narrow mechanical regime in which process stretch-growth was observed.

We identified a physiological response regime in which the application of external mechanical forces to astrocytic processes caused the cells to physically expand/elongate, meaning that they would have produced new intracellular constituents (e.g. plasma membrane, cytoskeleton,

organelles, etc.) and increased volume. This adaptation to the applied mechanical tension confirms that the cells remain physiologically active and viable. The mechanical regime that we identified should not be confused with numerous studies that have applied external mechanical forces to astrocytes in order to model nervous system injury, e.g. traumatic brain injury (TBI). Here, multiple studies have investigated the effects of ‘stretch injury’ on astrocytic responses, and have found that rapidly applied, i.e. millisecond (ms) to second (s) scale, large-magnitude mechanical stimulation may lead to a reactive astrogliosis and cell death *in vitro* (Ahmed *et al.*, 2000; Cullen *et al.*, 2007a, 2007b; Miller *et al.*, 2009). A notable difference between ‘stretch-injury’ models and our discovery of a growth-inducing stretch regime is the rate at which a displacement is applied. Previously, studies have shown that a strain magnitude of 10–50% applied over 10–500 ms is appropriate for simulating the biomechanics of TBI across a range of severities, and exposing 3D neuronal–astrocytic co-cultures to such loading regimes leads to neural cell death and reactive astrogliosis (Cullen *et al.*, 2006, 2007a, 2007b; Meaney *et al.*, 1995). For instance, when large-magnitude strain was applied at high strain rates (30 s^{-1} ; corresponding to 50% shear strain applied over 16.6 ms), significant cell death was observed, whereas at lower strain rates (1 s^{-1} and 10 s^{-1} ; corresponding to 50% shear strain applied over 500 ms or 50 ms, respectively) there was reduced cell death but significant astrocyte hypertrophy and hyperplasia (Cullen *et al.*, 2007a, 2007b; LaPlaca *et al.*, 2005). Additionally, in studies where astrocytes and neurons were subjected to stretch-injury in a two-dimensional (2D) paradigm *in vitro*, the application of 31%, 38% and 54% strain induced mitochondrial dysfunction as well as depletion of calcium ion stores, which were found to be more pronounced in astrocytes than neurons (Ahmed *et al.*, 2000). Across these *in vitro* studies of TBI-relevant mechanical loading, astrocytes may be more physiologically responsive to deformation than neurons (and becoming reactive, for instance). However, neurons have been shown to have lower thresholds for cell death following the application of high strain magnitude, high strain rate loading typical of TBI. This ‘injury response’ is in contrast to the ‘growth response’ featured in this paper, where astrocyte processes were found to be less resilient to stretch-growth than what was previously reported for axons (Pfister *et al.*, 2004).

A common result of major injury or disease in the CNS is the glial scar, comprised of reactive glial cells, in particular astrocytes. The glial scar not only acts as a physical barrier but also secretes factors that inhibit axons from regenerating through the injured area. Other studies have aimed to create constructs consisting of aligned astrocytic processes for neuroregeneration applications, most devised to guide axonal regeneration across the glial scar. For instance, aligned astrocytes have been generated via surface micropatterning, application of electric fields or by seeding in a matrix to bridge the glial scar (Alexander *et al.*, 2006; East *et al.*, 2010; Recknor *et al.*, 2004). In a recent study, astrocytes were aligned in a 3D collagen gel

Elongation of astrocyte processes for nervous system regeneration

in order to direct axon outgrowth following spinal cord injury (East *et al.*, 2010). When neurons were seeded into this construct, longer neurite outgrowth was seen in areas where astrocytes were aligned vs areas where they were not aligned. Additionally, these 3D aligned astrocyte constructs were compressed for implantation, and maintained neurite outgrowth (East *et al.*, 2010). Moreover, radial glia and immature glia have been of interest, as they may differentiate into neuronal or more mature glial lineages and developmentally serve as scaffolds along which neurons may migrate. Recapitulating this developmental process may prove beneficial for neuroregeneration. Recently, mature astrocytes were cultured on a micropatterned poly(methyl methacrylate) (PMMA) substrate, leading to a more immature, bipolar radial glia-like phenotype in a highly organized manner, akin to that during development (Mattotti *et al.*, 2012).

Additionally, freeze–thaw techniques and defined, serum-free culture of mature astrocytes were seen to lead to dedifferentiation of mature astrocytes into radial glia-like cells (Yu *et al.*, 2006). To alleviate the effects of the glial scar and permit axon guidance, the delivery of certain growth factors and/or enzymes, as well as cell transplantation into lesion sites, have been studied to promote regeneration. Recently, immature astrocytes along with chondroitinase-ABC were injected into a lesion site and induced axon regeneration beyond the distal edge of the lesion (Filous *et al.*, 2010). While these studies show promise, future studies will be required to assess the degree to which these techniques recapitulate developmental axonal pathfinding and neural migration tactics to effectively lead to neuroregeneration.

Overall, we have developed novel techniques to create aligned astrocyte processes spanning several mm as a

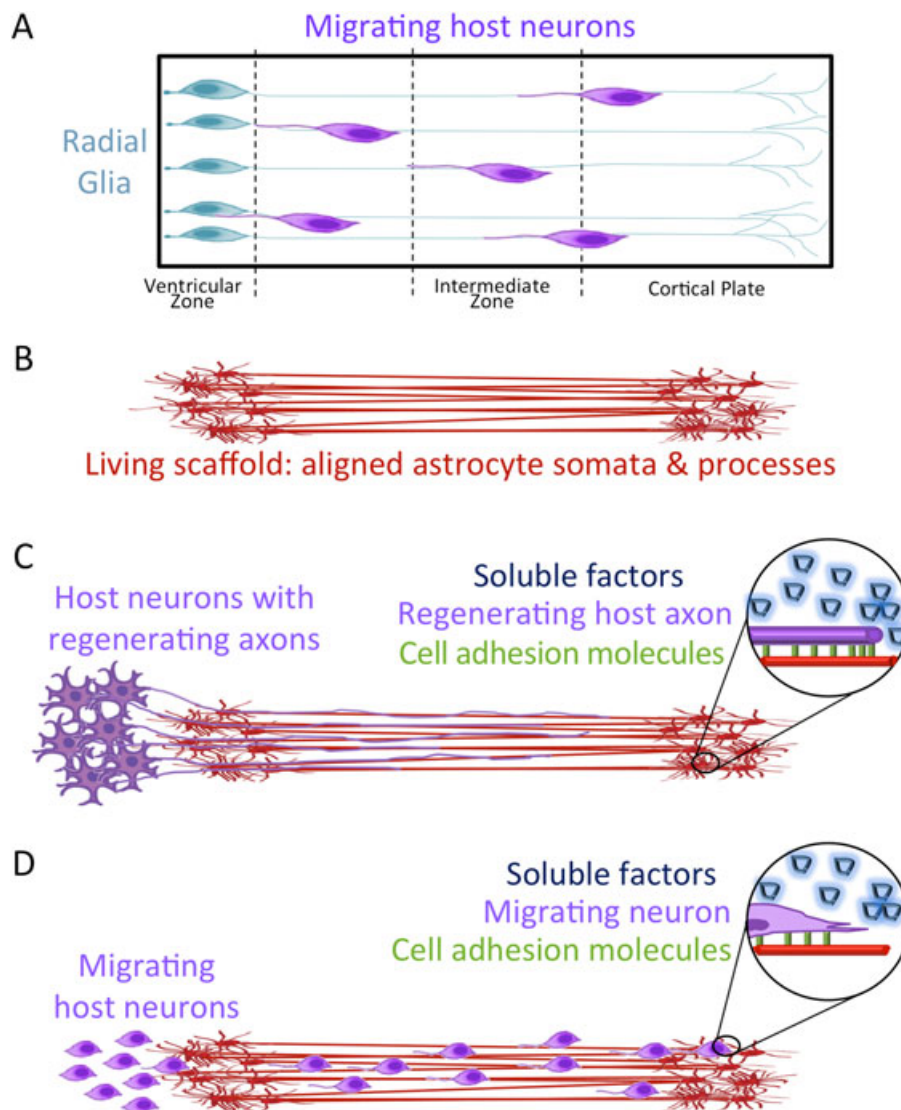


Figure 10. Concept: tissue-engineered living scaffolds comprised of aligned astrocytic somata and processes may promote nervous system regeneration. (A) During brain development, radial glia serve as natural ‘living scaffolds’ to guide immature neurons to the cortical layers. (B) Tissue-engineered astrocytic living scaffolds consisting of astrocyte somata and stretch-grown, aligned processes may be applied to (C) guide regenerating axons and/or (D) promote neuronal migration to a specified region. These processes are mediated by juxtacrine signalling, a concurrent and synergistic presentation of a panoply of cell-mediated haptotactic, chemotactic and neurotrophic cues

stepping stone to creating astrocytic 'living scaffolds' to facilitate nervous system regeneration following major injury or degeneration. Indeed, these stretch-grown astrocyte somata and processes may be utilized as 'living scaffolds' for CNS repair – specifically inducing neuronal precursor migration and/or axonal extension across regions of degeneration. Importantly, we found that these GFAP-positive elongated astrocytic processes were able to successfully promote neurite extension and neuronal migration directly along the stretched process. This demonstrates support and permissiveness for neuronal survival and outgrowth, and bodes well for future applications of this technology in neuroregeneration. To create 3D transplantable constructs consisting of our long, aligned astrocyte processes, we anticipate applying methodology for proteinaceous encapsulation and removal from culture *en masse*. Creating such 3D constructs for regenerative applications will entail either stretch-growth of encapsulated astrocyte networks or encapsulation of the astrocyte network after stretch-growth. Of note, we routinely encapsulate stretch-grown axonal constructs for transplantation using high-density collagen I matrix for stabilization and removal from culture (Huang et al., 2009; Pfister et al., 2006). Developmentally, neurons and their axons are guided via precisely orchestrated cell adhesion and soluble cues presented by cellular scaffolding. In the CNS, this largely occurs along immature radial glial cells that extend from the ventricular zone to the cortical plate (Figure 10a). We are currently evaluating the ability of 3D constructs containing mechanically grown, aligned glial processes (Figure 10b) to orchestrate a dual mechanism for regeneration: axonal pathfinding (Figure 10c) and neural cell migration (Figure 10d). The 3D living astrocytic scaffolds may also be used as test-beds to further elucidate mechanisms of neuroregeneration, in

particular cell migration and axonal pathfinding, as key cell–cell interactions and soluble factors involved in regeneration may be further studied using this system.

In summary, we have discovered a novel mechanical regime that may be applied to create aligned astrocytic processes spanning extreme lengths of up to 2.5 mm, with no evidence that greater lengths are not attainable. This technique marks an important step in structurally emulating radial glia and recapitulating a significant aspect of the CNS developmental programme. In particular, these novel constructs consisting of long-distance astrocytic processes offer an innovative method of creating an *in vitro* test-bed to study neurodevelopmental mechanisms in a reduced system. Moreover, this is a key enabling technology in developing tissue-engineered 'living scaffolds' that have the potential to mimic developmental mechanisms, to potentially drive the re-establishment of complex neural structures and axonal connections, potentially facilitating functional recovery following CNS neurotrauma or neurodegenerative disease.

Acknowledgements

Financial support was provided by the US Army Medical Research and Materiel Command through the Joint Warfighter Medical Research Program (Grant No. W81XWH-13-207004), the National Science Foundation (Graduate Research Fellowship No. DGE-1321851), the National Institutes of Health (NIH; Grant No. T32-NS043126), the Department of Veterans Affairs (RR&D Merit Review No. B1097-I), the Penn Medicine Neuroscience Center, and Penn's Center for Undergraduate Research and Fellowships.

Conflict of interest

The authors have declared that there is no conflict of interest.

References

- Ahmed SM, Rzigalinski BA, Willoughby KA et al. 2000; Stretch-induced injury alters mitochondrial membrane potential and cellular ATP in cultured astrocytes and neurons. *J Neurochem* **74**: 1951–1960.
- Alexander JK, Fuss B, Colello RJ. 2006; Electric field-induced astrocyte alignment directs neurite outgrowth. *Neuron Glia Biol* **2**: 93–103.
- Chen Y, Swanson RA. 2003; Astrocytes and brain injury. *J Cereb Blood Flow Metab* **23**: 137–149.
- Cullen DK, Simon CM, LaPlaca MC. 2007a; Strain rate-dependent induction of reactive astrogliosis and cell death in three-dimensional neuronal–astrocytic co-cultures. *Brain Res* **1158**: 103–115.
- Cullen DK, Stabenfeldt SE, Simon CM et al. 2007b; *In vitro* neural injury model for optimization of tissue-engineered constructs. *J Neurosci Res* **85**: 3642–3651.
- Cullen DK, Tang-Schomer MD, Struzyna LA et al. 2012; Microtissue engineered constructs with living axons for targeted nervous system reconstruction. *Tissue Eng A* **18**: 2280–2289.
- Cullen DK, Vukasinovic J, Glezer A et al. 2006; High cell density three-dimensional neural co-cultures require continuous medium perfusion for survival. *Conf Proc IEEE Eng Med Biol Soc* **1**: 636–639.
- Cullen DK, Vukasinovic J, Glezer A et al. 2007c; Microfluidic engineered high cell density three-dimensional neural cultures. *J Neural Eng* **4**: 159–172.
- Cullen DK, Wolf JA, Vernekar VN et al. 2011; Neural tissue engineering and biohybridized microsystems for neurobiological investigation *in vitro* (Part 1). *Crit Rev Biomed Eng* **39**: 201–240.
- East E, de Oliveira DB, Golding JP et al. 2010; Alignment of astrocytes increases neuronal growth in three-dimensional collagen gels and is maintained following plastic compression to form a spinal cord repair conduit. *Tissue Eng A* **16**: 3173–3184.
- Fawcett JW, Asher RA. 1999; The glial scar and central nervous system repair. *Brain Res Bull* **49**: 377–391.
- Filous AR, Miller JH, Coulson-Thomas YM et al. 2010; Immature astrocytes promote CNS axonal regeneration when combined with chondroitinase ABC. *Dev Neurobiol* **70**: 826–841.
- Gabella B, Hoffman RE, Marine WW et al. 1997; Urban and rural traumatic brain injuries in Colorado. *Ann Epidemiol* **7**: 207–212.
- Gaul G, Lubbert H. 1992; Cortical astrocytes activated by basic fibroblast growth factor secrete molecules that stimulate differentiation of mesencephalic dopaminergic neurons. *Proc Biol Sci* **249**: 57–63.
- Harris JP, Struzyna LA, Murphy PL, Adewole DO, Kuo E, Cullen DK. 2016; Advanced biomaterial strategies to transplant

Elongation of astrocyte processes for nervous system regeneration

- performed micro-tissue engineered neural networks into the brain. *J Neural Engineering* **13**(1): 016019.
- Hatten ME, Mason CA. 1990; Mechanisms of glial-guided neuronal migration *in vitro* and *in vivo*. *Experientia* **46**: 907–916.
- Huang JH, Cullen DK, Browne KD *et al.* 2009; Long-term survival and integration of transplanted engineered nervous tissue constructs promotes peripheral nerve regeneration. *Tissue Eng A* **15**: 1677–1685.
- Irons HR, Cullen DK, Shapiro NP *et al.* 2008; Three-dimensional neural constructs: a novel platform for neurophysiological investigation. *J Neural Eng* **5**: 333–341.
- Jacobs JR, Goodman CS. 1989; Embryonic development of axon pathways in the *Drosophila* CNS. I. A glial scaffold appears before the first growth cones. *J Neurosci* **9**: 2402–2411.
- Jaeger CB. 1988; Plasticity of astroglia: evidence supporting process elongation by 'stretch'. *Glia* **1**: 31–38.
- Joosten EA, Gribnau AA. 1989; Astrocytes and guidance of outgrowing corticospinal tract axons in the rat. An immunocytochemical study using anti-vimentin and anti-glial fibrillary acidic protein. *Neuroscience* **31**: 439–452.
- LaPlaca MC, Cullen DK, McLoughlin JJ *et al.* 2005; High rate shear strain of three-dimensional neural cell cultures: a new *in vitro* traumatic brain injury model. *J Biomech* **38**: 1093–1105.
- Leavitt BR, Hernit-Grant CS, Macklis JD. 1999; Mature astrocytes transform into transitional radial glia within adult mouse neocortex that supports directed migration of transplanted immature neurons. *Exp Neurol* **157**: 43–57.
- Liverman, C.T. & Institute of Medicine (U.S.). Committee on Spinal Cord Injury 2005; *Spinal cord injury: progress, promise, and priorities*, National Academies Press: Washington, DC.
- Mattotti M, Alvarez Z, Ortega JA *et al.* 2012; Inducing functional radial glia-like progenitors from cortical astrocyte cultures using micropatterned PMMA. *Biomaterials* **33**: 1759–1770.
- McCarthy KD, de Vellis J. 1980; Preparation of separate astroglial and oligodendroglial cell cultures from rat cerebral tissue. *J Cell Biol* **85**: 890–902.
- Meaney DF, Smith DH, Shreiber DI *et al.* 1995; Biomechanical analysis of experimental diffuse axonal injury. *J Neurotrauma* **12**: 689–694.
- Miller WJ, Leventhal I, Scarsella D *et al.* 2009; Mechanically induced reactive gliosis causes ATP-mediated alterations in astrocyte stiffness. *J Neurotrauma* **26**: 789–797.
- Pfister BJ, Iwata A, Meaney DF *et al.* 2004; Extreme stretch growth of integrated axons. *J Neurosci* **24**: 7978–7983.
- Pfister BJ, Iwata A, Taylor AG *et al.* 2006; Development of transplantable nervous tissue constructs comprised of stretch-grown axons. *J Neurosci Methods* **153**: 95–103.
- Pixley SK, Nieto-Sampedro M, Cotman CW. 1987; Preferential adhesion of brain astrocytes to laminin and central neurites to astrocytes. *J Neurosci Res* **18**: 402–406.
- Recknor JB, Recknor JC, Sakaguchi DS, *et al.* 2004; Oriented astroglial cell growth on micropatterned polystyrene substrates. *Biomaterials* **25**: 2753–2767.
- Scemes E, Spray DC. 2011; *Astrocytes: Wiring the Brain*. Taylor & Francis: Boca Raton, FL, USA, 400 pp.
- Smith DH. 2009; Stretch growth of integrated axon tracts: extremes and exploitations. *Prog Neurobiol* **89**: 231–239.
- Stiles J, Jernigan TL. 2010; The basics of brain development. *Neuropsychol Rev* **20**: 327–348.
- Struzyna LA, Katiya KS, Cullen DK. 2014; Living scaffolds for neuroregeneration. *Curr Opin Solid State Mater Sci* **18**: 308–318.
- Struzyna L, Harris J, Katiyar K *et al.* 2015a; Restoring nervous system structure and function using tissue engineered living scaffolds. *Neural Regen Res* **10**: 679.
- Struzyna LA, Wolf JA, Mietus CJ *et al.* 2015b; Rebuilding brain circuitry with living micro-tissue engineered neural networks. *Tissue Eng A* **21**: 2744–2756.
- Vukasinovic J, Cullen DK, LaPlaca MC *et al.* 2009; A microperfused incubator for tissue mimetic 3D cultures. *Biomed Microdevices* **11**: 1155–1165.
- Yiu G, He Z. 2006; Glial inhibition of CNS axon regeneration. *Nat Rev Neurosci* **7**: 617–627.
- Yu T, Cao G, Feng L. 2006; Low-temperature induced dedifferentiation of astrocytes. *J Cell Biochem* **99**: 1096–1107.
- Zhou HF, Lee LH, Lund RD. 1990; Timing and patterns of astrocyte migration from xenogeneic transplants of the cortex and corpus callosum. *J Comp Neurol* **292**: 320–330.